IEEE Access
Multidisciplinary ⋮ Rapid Review ⋮ Open Access Journal

Received April 2, 2022, accepted May 11, 2022, date of publication May 17, 2022, date of current version May 26, 2022.

Digital Object Identifier 10.1109/ACCESS.2022.3175841

User-Transformer Connectivity Relationship Identification Based on Knowledge-Driven Approaches

LAI ZHOU, FUJUN WEN, XIANFU YANG, AND YUMING ZHONG
School of Intelligent Manufacturing, Guangzhou Panyu Polytechnic, Guangzhou 511483, China

Corresponding author: Fujun Wen (11805914@qq.com)

This work was supported in part by the Science and Technology Project Foundation of Guangzhou Panyu Polytechnic, China, under Grant 2022KJ10.

ABSTRACT Accurate user-transformer connectivity relationship (UTCR) plays a key role in fine management of low-voltage distribution network (LVDN) i.e., load expansion, line loss management, and electrical service restoration after outage. Limited data and low discriminability and noise in data increase the difficulty to identify UTCR for the existing data analytics methods. To overcome these hurdles, this paper proposes a novel UTCR algorithm which combining the data preprocessing with multi-dimensional priori knowledge based on voltage characteristics in LVDN. Firstly, the prior knowledge related to UTCR are refined on account of voltage correlation characteristics of users at different locations to provide theoretical foundation. Then, Z-score and principal component analysis are combined to standardize and extract features from the original voltage data to magnify the differences between data and reduce the impact of data noise. Further, on the basis of the prior knowledge of voltage correlation characteristics, a knowledge-driven identification model is proposed to identify users with wrong UTCR and their real UTCR. Finally, the performance of the proposed algorithm is verified on simulated LVNDs. The comparison analysis between the proposed method and other published methods and the impact of the number of principal components on the identification accuracy are also investigated. The results indicate that the proposed method achieves higher recognition accuracy than other published methods with low discriminability and noise in data.

INDEX TERMS User-transformer connectivity relationship identification, low-voltage distribution network, data pre-processing, voltage correlation characteristics, knowledge-driven approaches.

I. INTRODUCTION

The massive use of fossil fuels has two drawbacks: resource depletion and climate crisis, which violates the sustainable development goal. To tackle this problem, many countries around the world have taken carbon neutrality into the development plan [1], [2]. Under this background, the penetration level of new equipment, i.e., rooftop photovoltaic, electric vehicle, and energy storage in LVDN increases gradually [3]–[5]. The development of these devices can effectively alleviate the pressure of environmental pollution and energy tension, but it has brought impacts and challenges to the safe operation and power supply quality of LVDN [6], [7]. In order to fully dig the potential of distributed energy resources meanwhile operating the grid in an efficient and reliable manner, a high-level operation and maintenance management in LVDN is needed [8]. Of which, accurate low-voltage physical topology connection information is a vital foundation to support the intelligent construction of LVDN [9], [10]. Low-voltage topological connections include the connections between distribution transformers, phase sequences, feeders and users. This paper focus on user-transformer connectivity relationship (UTCR) identification, defined as the connection relationship between the terminal user's electricity meter and the distribution transformer of LVDN.

With the development of economy and the continuous advancement of urbanization, the number of users in LVDN increases rapidly, and UTCR changes frequently. However, affected by low efficiency of investigation and untimely

The associate editor coordinating the review of this manuscript and approving it for publication was Ghufran Ahmed.

update of information, the UTCR information that utilities have usually existed many errors. Accurate UTCR is the key to load expansion, line loss management, electrical service restoration after outage, line transformation and other services, and is also the premise to accurately identify the connections among phase sequences, feeders and users [11], [12]. The traditional methods relying on manual techniques and signal injection devices are inefficient and need high investment cost, which is hard to afford for grid companies. Besides, it cannot update topology information automatically. Therefore, it is important to study the automatic recognition technology for UTCR.

Nowadays, deploying smart meters in LVDN is development trend [13]. In particular, China has achieved 100% penetration of smart meters in LVDN since 2019. In this context, a large amount of users' electricity consumption data and network operation data can be obtained. New approaches are intensively investigated to apply the data acquired by smart meters for the planning and operation of distribution systems, i.e., non-technical loss detection, non-intrusive load monitoring, power quality assessment, fault location [14], [15]. Similarly, with the advantages of low cost and convenient, new methods using smart meters data have been widely employed for topology connectivity identification in LVDN [10], [16]–[18]. [16] and [10] focus on the topology and parameter estimation for LVDN with smart meters. [17], [18] are methodologies utilizing voltage data and current data from smart meters and transformers to recognize phase connectivity relationship of users. All of the above studies need accurate UTCR as a priori knowledge. By the data types they require, the existing methods for UTCR recognition could be categorized into five sets.

1) Power data: in [11], based on the power data of users and transformers, a quadratic optimization model was established to minimize the network loss fluctuation rate to determine UTCR. In [12], the combination of linear regression and a Dirichlet-Categorical allocation model sampled with Markov chain Monte Carlo was proposed to track and identify low-voltage topology changes, in which the UTCR information was included. In [19], a de-noised differential evolution-based method was proposed for topology identification.

2)Current data: in [20], the high-frequency features from current data were extracted by Discrete Fourier Transform and Inverse Discrete Fourier Transform. Further, an optimization model based on Kirchhoff's law of current was constructed to get UTCR.

3) Voltage data: in [21], performing Fisher Z transform on Pearson correlation coefficient matrix based on the total harmonic voltage were proposed to determine low-voltage connectivity. In [22], voltage correlation factors between all customers were calculated, and the users with strong correlations were assumed to be on the same transformer. In [23], voltage curve correlation analysis between users and low-voltage buses was employed to verify UTCR.

4) GIS data: in [24], new procedures that exploit the graph theory and data structure properties were presented to detect and correct errors in models of LVDN.

5) Multi-source data: in [25], regression and basic voltage drop relationships based on power data and voltage data were employed to generate secondary connectivity and impedance models. In [26], principal component analysis and independent component analysis were employed to extract features form voltage data. Then, the Pearson correlation analysis between the users' total current and transfer's current was used to realize UTCR recognition. In [27], a two-stage approach for UTCR was proposed based on voltage data and power data. At first stage, correlation analysis was employed to ensure transformers with errors in UTCR, then a linear regression formulation was built to correct the errors. In [28], a multiple linear regression model using voltage and power data of customers meters was established to estimate topology, line parameters, and customer and line phasing connections in LVDN.

The methods in the first and second categories using current and power data are suitable for scenarios where consumers' power consumption characteristics are obvious and there is no electricity theft and unmetered load. However, in practice, it is also common that the obtained power consumption data of consumers is incomplete and cannot fully reflect the power consumption of LVDN, resulting from poor communication quality, human error, unregistered meters, and electricity theft. The methods in the fourth category need GIS data. GIS data for LVDN are not available for many areas such as China. The application scenarios of the methods using GIS data are limited. For the methods based on linear regression in the fifth category, on the one hand, it requires a lot of data, including the voltage, active and reactive power data of all users in LVDN. Nevertheless, it is difficult to provide complete data in many areas, which reduces the effective application scenarios of the methods. On the other hand, there are many parameters involved in the regression model, and parameter thresholds need to be set. How to select appropriate parameter thresholds increases the difficulty of applying the methods.

Voltage-based methods in the third category have strong robustness to electricity theft and unmetered load. The voltage correlation characteristics analysis among users or that between users and transformer was employed in the existing voltage-based methods individually. However, the volage correlation characteristics of users depend on their location. There may be contradictory correlation characteristics between users located in different locations. Hence, the existing voltage-based methods only using one correlation characteristic are not sufficient to accurately identify UTCR.

Besides, the existing voltage-based methods lack data preprocessing, and have less robustness to data discrimination and noise. In practice, the voltage data collected from LVDN with three-phase unbalanced governance tend to be centralized. And the difference between user's voltage characteristics is small, which affects the accuracy of the algorithm.

Moreover, affected by meter measurement errors and communication problems, the data collected by smart meters often contains some noise. Low discriminability and noise in data affect the performance of the existing voltage-based methods.

In conclusion, despite its importance, how to identify UTCR accurately with voltage data and enhance the robustness of the identification method to data discrimination and noise has not been well investigated. To overcome these hurdles, this paper introduces data preprocessing and multi-dimensional priori knowledge in UTCR algorithm based on voltage characteristics in LVDN. The improvements on existing voltage correlation approaches include:

1) The voltage correlation characteristics of users at different locations are deduced, and the prior knowledge related to UTCR are further refined, which provides a theoretical basis for the recognition algorithm.
2) Z-score and principal component analysis are combined to standardize and extract features from the original voltage data to magnify the differences between data and reduce the impact of data noise.
3) Based on the prior knowledge of voltage correlation characteristics, a knowledge-driven identification model is proposed to identify users with wrong UTCR and their real UTCR.
4) Compared with the existing methods, the proposed algorithm achieves higher UTCR identification accuracy, and has better robustness to data discrimination and noise.

The rest of this paper is organized as follows. Section II describes the problem formulation. Section III deduces the prior knowledge of UTCR based on voltage data. Section IV describes the mathematical model of the proposed UTCR algorithm. The tests and results are illustrated in Section V. At last, Section VI presents the conclusion of the study and the future work.

II. PROBLEM FORMULATION

Distribution system is the final portion of electric power system and feeds power from transmission system to users. It includes medium-voltage distribution network and LVDN. At present, the topology of medium-voltage distribution network is available for grid companies. The information that utilities have about LVDN is limited to UTCR which defined as the connectivity between meters and transformer.

An illustration of a simple distribution network is presented in Fig.1. It can be seen from Fig.1, the meters M1, M2, M3, and M4 are powered by the distribution transformer T1. Hence, these meters are considered to belong to LVDN#1. Similarly, the meters M5, M6, M7, and M8 are powered by the distribution transformer T2, these users are considered to belong to LVDN#2. Smart meters located in consumer side measure consumers' power consumption, voltage, current, power factor, and other data at regular time intervals.

Data concentrator units (DCU) are installed near the distribution transformer in LVDN to collect smart meter data through wireless and power line communication [12]. Terminal meters installed at the low-voltage buses of distribution transformer measure the total power consumed, voltage, current, power factor of each low-voltage bus. As a result, the power consumption, voltage, current, power factor, and other data of consumer and transformer in LVDN can be available for Grid company by DCU and terminal meters. DCU stores the ID of smart meters needed to be collected. This ID information can be regarded as the UTCR that power grid companies can obtain at present. Ideally, DCU contains only the ID information of all meters powered by the LVDN which it located in. However, in practice, it is quite common that the ID information of smart meters in the DCU is not consistent with the actual UTCR. This may have the following situations:

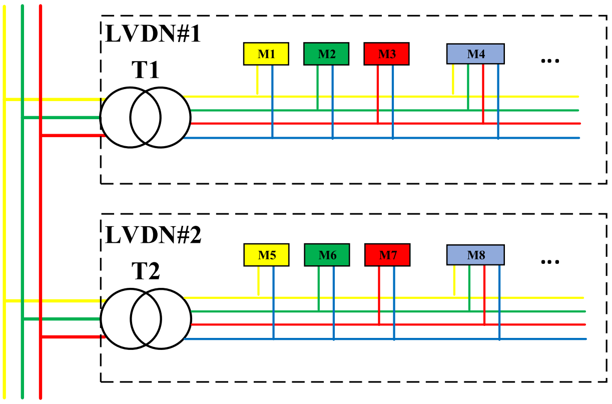

FIGURE 1. Illustration of a simple distribution network.

1) DCU contains the ID information of part of meters powered by the LVDN which it located in;
2) DCU contains not only the ID information of all meters powered by the LVDN which it located in, but also the ID information of meters in other LVDN;
3) DCU contains not only the ID information of part of meters powered by the LVDN which it located in, but also the ID information of meters in other LVDN.

The reasons for the discrepancy between the information in DCU and the actual UTCR include: 1) due to LVDN operation mode adjustment, some users are transferred to other LVDN, but the ID information in the DCU is not updated in time; 2) in the complex wiring area, it is difficult to distinguish UTCR, and the wrong ID information of meters was manually recorded. Accurate UTCR is not only the basis for the refinement of LVDN line loss management and energy saving, but also affects the accurate recognition of the following full topology of LVDN. Hence, it is very important and necessary to investigate how to identify UTCR.

III. PRIOR KNOWLEDGE RELATED TO UTCR

Under the constraints of power flow, voltage and current data between nodes in LVDN are correlated in time and space. This section first deduces the temporal and spatial

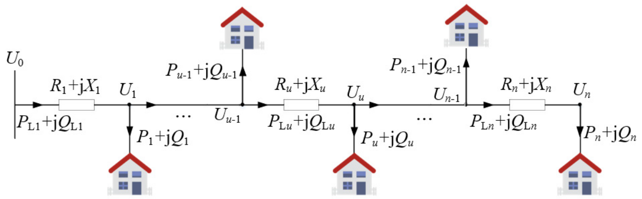

FIGURE 2. **Illustration of a feeder line in LVDN.**

characteristics of measured data in LVDN from the node voltage calculation formula. On this basis, the prior knowledge related to UTCR is further analyzed. The details are elaborated as follows.

In practice, the service drop line between feeder and household is short. Hence, the voltage drop between users and feeder line is ignored in the theoretical derivation to better understand the voltage characteristics among users. Moreover, the reverse power flow is not consideredin the theoretical derivation. The illustration of a feeder line in LVDN is depicted in Fig.2.

1) Voltage space characteristic analysis

As shown in Fig.2, on the basis of voltage drop formula, the voltage of node u at time t, U_u^t can be approximated by

$$\begin{aligned} U_u^t &\approx U_{u\,-\,1}^t - \frac{R_u P_{\mathrm{L}u}^t + X_u Q_{\mathrm{L}u}^t}{U_{u-1}^t} \\ &\approx U_{u\,-\,2}^t - \frac{R_{u-1} P_{\mathrm{L}u-1}^t + X_{u-1} Q_{\mathrm{L}u-1}^t}{U_{u-2}^t} \\ &\quad - \frac{R_u P_{\mathrm{L}u}^t + X_u Q_{\mathrm{L}u}^t}{U_{u-1}^t} \\ &\approx U_0^t - \frac{R_1 P_{\mathrm{L}1}^t + X_1 Q_{\mathrm{L}1}^t}{U_0^t} - \frac{R_2 P_{\mathrm{L}2}^t + X_2 Q_{\mathrm{L}2}^t}{U_1^t} \cdots \\ &\quad - \frac{R_u P_{\mathrm{L}u}^t + X_u Q_{\mathrm{L}u}^t}{U_{u-1}^t} \\ &\approx U_0^t - \sum_{i=1}^{u} \frac{R_i P_{\mathrm{L}i}^t + X_i Q_{\mathrm{L}i}^t}{U_{i-1}^t}, \quad u = 1, 2, \cdots, n \end{aligned} \tag{1}$$

where, U_0^t is the voltage of low-voltage bus at time t, U_{u-1}^t is the voltage of node u-1 at time t, R_u and X_u are the resistance and reactance of line u, respectively, $P_{\mathrm{L}u}^t$ and $Q_{\mathrm{L}u}^t$ are the active power transmitted by line u at time t, respectively, including the active and reactive power loss of line u, R_i and X_i are the resistance and reactance of line i, respectively, $P_{\mathrm{L}i}^t$ and $Q_{\mathrm{L}i}^t$ are the active power transmitted by line i at time t, respectively, including the active and reactive power loss of line i, n is the total number of nodes in the feeder. $(R_i\ P_{\mathrm{L}i}^t + X_i Q_{\mathrm{L}i}^t)\,/U_{i-1}^t$ is the voltage drop at line i in terms of power and voltage.

Further, the voltage drop of adjacent nodes at time t, $\Delta G^t u$ is given by

$$\Delta G_u^t = U_{u+1}^t - U_u^t \approx -\frac{R_{u+1} P_{\mathrm{L}u+1}^t + X_{u+1} Q_{\mathrm{L}u+1}^t}{U_u^t} < 0 \tag{2}$$

The influencing factors of node voltage and voltage drops are shown in (1) and (2), respectively. According to (1) and (2), voltage space characteristics are summarized as follow:

1) U_u^t depends on the voltage of low-voltage bus (U_0^t), the total load (P_{Lj}^t and Q_{Lj}^t) and a combination of distance of lines between the consumer and the source node i.e., R_i, i=1, 2, …u.
2) Without consideration of reverse power flow in LVDN, the voltage amplitude of the nodes along the line gradually decreases.

2) Voltage time characteristic analysis

According to (1), the voltage changes of node u at adjacent time ΔU_u^t is given by

$$\begin{aligned} \Delta U_u^t = U_u^{t+1} - U_u^t &\approx U_0^{t+1} - U_0^t \\ &\quad - \sum_{i=1}^{u} \frac{R_i P_{\mathrm{L}i}^{t+1} + X_i Q_{\mathrm{L}i}^{t+1}}{U_{i-1}^{t+1}} \\ &\quad + \sum_{i=1}^{u} \frac{R_i P_{\mathrm{L}i}^{t} + X_i Q_{\mathrm{L}i}^{t}}{U_{i-1}^{t}} u = 1, 2, \cdots, n \end{aligned} \tag{3}$$

where, U_u^t and U_u^{t+1} are the voltage of node u at time t and $t+1$, respectively, $U_0^t$and $U_0^{t+1}$are the voltage of low-voltage bus at time t and $t+1$, respectively, $P_{\mathrm{L}j}^t$ and $Q_{\mathrm{L}j}^t$ are the active power transmitted by line j at time t, respectively, including the active and reactive power loss of line j.

According to (3), voltage time characteristics are summarized as follow:

1) ΔU_u^t depends on the variation characteristic of the total load and the voltage of low-voltage bus, and a combination of distance of lines between the consumer and the source node i.e., R_i, i=1, 2, …u.

Further, the prior knowledge related to UTCR are refined on the basis of the voltage space and time characteristics. For nodes near the low-voltage bus, the line distance from it to the low-voltage bus is short. Then, the distance of each line between these nodes and the low-voltage bus are also short. Hence, resistance (R_i) and reactance (X_i) of each line between these nodes and the low-voltage bus are small. Therefore, for nodes near the low-voltage bus, we assume

$$-\sum_{i=1}^{u} \frac{R_i P_{\mathrm{L}i}^{t+1} + X_i Q_{\mathrm{L}i}^{t+1}}{U_{i-1}^{t+1}} + \sum_{i=1}^{u} \frac{R_i P_{\mathrm{L}i}^{t} + X_i Q_{\mathrm{L}i}^{t}}{U_{i-1}^{t}} \approx 0 \tag{4}$$

Plugging (4) into (3), we obtain $\Delta U_u^t \approx \Delta U_0^t$. Due to the differences in the voltage of low-voltage bus and the total load of different LVDN, the users near the low-voltage bus have the greatest voltage similarity to the bus which they connect to. For example, the voltage curves of M1 and M5 in Fig.1 are the most similar to that of the low-voltage bus of T1 and T2, respectively.

The Person correlation coefficients of voltage profiles (PCCVP) are introduced to describe the similarity among voltage profiles in this study. The more similar the voltage profiles, the greater the PCCVP. The calculation formula is as follows:

$$\rho_{rs} = \frac{\mathrm{cov}(r, s)}{\sigma_r \sigma_s} = \frac{E[(X - \mu_r)(Y - \mu_s)]}{\sigma_r \sigma_s} \tag{5}$$

where, ρ_{rs} is the Pearson correlation coefficient between voltage series; $\mathrm{cov}(r,s)$ is the covariance of the voltage series of node r and s; σ_r and σ_s are the standard deviations of the voltage series of node r and s, respectively; X and Y are the voltage series of node r and s; μ_r and μ_s are the mean values of X and Y, respectively.

Therefore, for users close to distribution transformer, the PCCVP between them and the low-voltage bus can be compared to determine their UTCR. The prior knowledge related to UTCR is summarized as follows:

Prior knowledge 1: For the users near distribution transformer, the PCCVP value between them and the low-voltage bus to which they are connected is the highest among low-voltage buses

However, for nodes far away from the low-voltage bus, affected by the total load variation and long line distance, ΔU_u^t could be significantly different from ΔU_0^t. The voltage profile similarity between the nodes far away from distribution transformer and the low-voltage bus would be low. It's uncertain which low-voltage bus has the largest PCCVP value with them. In other words, the transformer connectivity of low-voltage bus which has the largest CCVP value to them may be same as them or not, on a case-by-case basis. Hence, it's hard to determine the UTCR of users far away from the low-voltage bus by comparing PCCVP between them and low-voltage buses.

According to the voltage time characteristics analyzed in above, the voltage changes of node u at adjacent time depends on the variation characteristic of the total load and the voltage of low-voltage bus, and a combination of distance of lines between the consumer and the source node. Due to the differences in the voltage of low-voltage bus and the total load of different LVDN, the voltage correlation between users will show different characteristics when they connect to different LVDN and phase sequence. Let Ω_k be the PCCVP between user k and other users, as described as below.

$$\Omega_k = \{\rho_{k1}, \rho_{k2}, \ldots, \rho_{kl}, \ldots, \rho_{kK}\} \tag{6}$$

where, ρ_{kl} is the PCCVP between user k and user l, K is the number of users.

The following situations exist among users in different LVDN:

1) The PCCVP of users in the same phase is strong, while that of users in different phases is weak. Therefore, the PCCVP sequence between users connected to same LVDN will show significant fluctuation, which means the standard deviation of PCCVP sequence is large. Users in other LVDN have weak voltage correlation with users connected to same LVDN. Therefore, the standard deviation of PCCVP sequence between users in other LVDN and users connected to same LVDN is small.
2) The PCCVP between users connected to same LVDN is strong, while that between users in other LVDN and users connected to same LVDN is weak. Therefore, the mean value of PCCVP sequence between users connected to same LVDN is large, while the mean value of PCCVP sequence between users in other LVDN and users connected to same LVDN is small.

The above two characteristics can be used to determine the UTCR of users far from low-voltage bus, and the prior knowledge related to UTCR is summarized as follows:

Prior knowledge 2: The standard deviation and mean of PCCVP sequence between users connected to same LVDN are large, while that between users in other LVDN and users connected to same LVDN is small.

The above prior knowledge is derived from the node voltage formula in the power grid. Since the node voltage formula is freely available, there is no cost to provide this prior knowledge.

IV. KNOWLEDGE-DRIVEN UTCR IDENTIFICATION ALGORITHM

Knowledges in this section are the prior knowledge related to UTCR which are deduced in Section III. Knowledge factor ϑ is defined as empirical rules derived from knowledge, and knowledge factor ϑ can be expressed as:

$$\vartheta : \{\text{if } M \text{ then } N\} \tag{7}$$

Formula (7) is an empirical rule of causal logic that if M is true, then N is true. M is the conditional event, which is the triggering condition of the knowledge factor. In this paper, conditional event can be set as the voltage correlation between multiple users, the convergence degree of node spatial location distribution or the similarity of high frequency components of load current and other indicators exceeding the threshold. N is the conclusion event, representing the empirical judgment under the truth of the conditional event M, such as the judgment of topological relations including upstream and downstream relationship, hierarchical relationship and position relationship of nodes. Knowledge-based UTCR identification algorithm is established in this section based on the prior information in Section III. The input data in the proposed method include the voltage curves of consumer and low-voltage buses in LVDNs to be recognized. The output result is user-transformer connectivity.

The flowchart for the proposed knowledge-driven UTCR identification algorithm is presented in Fig.3. As shown in Fig.3, the proposed method consists of two parts. The first part is the data pre-processing. In this part, Z-score and principal component analysis are combined to standardize and extract features from the original voltage data to magnify the differences between data and reduce the impact of data noise. The second part is the recognition for UTCR, in which **Prior knowledge 1** and **2** are employed to verify the UTCR

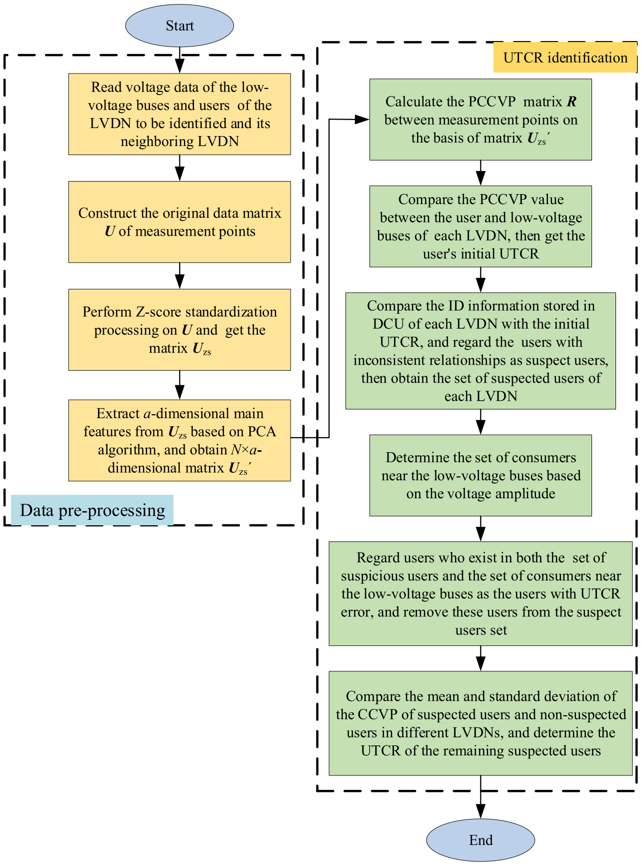
Start
Data pre-processing
Read voltage data of the low-voltage buses and users of the LVDN to be identified and its neighboring LVDN
Construct the original data matrix U of measurement points
Perform Z-score standardization processing on U and get the matrix U_{zs}
Extract a-dimensional main features from U_{zs} based on PCA algorithm, and obtain N×a-dimensional matrix U_{zs}'
UTCR identification
Calculate the PCCVP matrix R between measurement points on the basis of matrix U_{zs}'
Compare the PCCVP value between the user and low-voltage buses of each LVDN, then get the user's initial UTCR
Compare the ID information stored in DCU of each LVDN with the initial UTCR, and regard the users with inconsistent relationships as suspect users, then obtain the set of suspected users of each LVDN
Determine the set of consumers near the low-voltage buses based on the voltage amplitude
Regard users who exist in both the set of suspicious users and the set of consumers near the low-voltage buses as the users with UTCR error, and remove these users from the suspect users set
Compare the mean and standard deviation of the CCVP of suspected users and non-suspected users in different LVDNs, and determine the UTCR of the remaining suspected users
End

FIGURE 3. **Flowchart of the knowledge-driven UTCR identification algorithm.**

of users near to low-voltage buses and users far away from low-voltage buses.

A. DATA STANDARDIZATION AND MAIN FEATURE EXTRACTION

In practice, the voltage data collected from LVDN with three-phase unbalanced governance tend to be centralized. And the difference between user's voltage characteristics is small, which affects the accuracy of the algorithm. Data standardization process, i.e., Z-score standardization is employed to improve the robustness of the proposed method on data discrimination. Moreover, affected by meter measurement errors and communication problems, the data collected by smart meters often contains some noise. Besides, a long period of data is also required to describe the overall law of voltage for all users in the LVDN. In order to reduce the influence of noise and time complexity of the algorithm, dimensionality reduction technique is used to retain the main characteristics of the voltage data. Of which, the principal component analysis (PCA) algorithm is introduced, since it has better performance in topology recognition compared with other dimensionality reduction technique, i.e., T-SNE.

1) Z-score standardization processing

Voltage correlation characteristics are used for UTCR recognition. Hence, in the data re-processing, it is expected to retain the data distribution characteristics in the original data set. In addition, there are differences in voltage fluctuation characteristics between users located in different phases, and the influence of statistical variance needs to be eliminated. As a feature scaling method, Z-Score standardization transforms the original data into a distribution with a mean value of 0 and a standard deviation of 1. Z-Score standardization does not change the characteristics of data distribution, de-averaging, and standardized variance, which can satisfy the data processing requirements in UTCR recognition.

The smart meters located on low-voltage buses and user side are defined as the metering point. The original voltage data matrix $\boldsymbol{U}$ is constructed based on the voltage data of the low-voltage buses and user of the LVDN to be identified and its neighboring LVDN, $\boldsymbol{U}$=[$\boldsymbol{U}_{L1}$; $\boldsymbol{U}_{L2}$; …; $\boldsymbol{U}_{Le}$; $\boldsymbol{U}_{C1}$; $\boldsymbol{U}_{C2}$; …; $\boldsymbol{U}_{Ce}$], where $\boldsymbol{U}_{L1}$ and $\boldsymbol{U}_{C1}$ respectively represent the voltage matrix of the low-voltage buses and users of the first LVDN, as shown in eq.(8) and eq.(9), e represents the total number of LVDN.

$$U_{\mathrm{L1}} = \begin{bmatrix} u^{1}_{\mathrm{L1A}} & u^{2}_{\mathrm{L1A}} & \cdots & u^{T}_{\mathrm{L1A}} \\ u^{1}_{\mathrm{L1B}} & u^{2}_{\mathrm{L1B}} & \cdots & u^{T}_{\mathrm{L1B}} \\ u^{1}_{\mathrm{L1C}} & u^{2}_{\mathrm{L1C}} & \cdots & u^{T}_{\mathrm{L1C}} \end{bmatrix} \tag{8}$$

$$U_{\mathrm{C1}} = \begin{bmatrix} u^{1}_{\mathrm{C11}} & u^{2}_{\mathrm{C11}} & \cdots & u^{T}_{\mathrm{C11}} \\ u^{1}_{\mathrm{C12}} & u^{2}_{\mathrm{C12}} & \cdots & u^{T}_{\mathrm{C12}} \\ \vdots & \vdots & \vdots & \vdots \\ u^{1}_{\mathrm{C1}f} & u^{2}_{\mathrm{C1}f} & \cdots & u^{T}_{\mathrm{C1}f} \end{bmatrix} \tag{9}$$

where, $u^{T}_{\mathrm{L1\ A}}$, $u^{T}_{\mathrm{L1\ B}}$ and $u^{T}_{\mathrm{L1\ C}}$ represent the voltage values of low-voltage bus of phase A, B and C in the first LVDN at time T, respectively; $u^{T}_{\mathrm{C1}f}$ represents the voltage of the f-th user at time T in the first LVDN; f is the total user ID number in the DCU of the first LVDN.

The Z-Score standardization calculation formula for voltage data of metering points is shown as below.

$$U^{t\prime}_{u} = \frac{U^{t}_{u} - \mu(U^{t}_{\Phi})}{\sigma(U^{t}_{\Phi})}, u \in \Phi \tag{10}$$

where, $U^{t\prime}_{u}$ represents the Z-Score standard value of the $u-$th metering point's voltage at time t, U^{t}_{Φ} is a column vector, including the voltage value of all metering points at time t, $\mu(U^{t}_{\Phi})$ represents the average voltage value of all metering points at time t, $\sigma(U^{t}_{\Phi})$ represents the voltage standard deviation of all measurement points at time t, F is the set of measurement points.

Let $U^{t\prime}_{\Phi}$ be the data set of measuring points standardized by Z-Score at time t. Then, the standardized voltage data set of measuring points $\boldsymbol{U}_{zs}$can be expressed as below.

$$U_{zs} = [U^{1\prime}_{\Phi}, U^{2\prime}_{\Phi}, \cdots, U^{T\prime}_{\Phi}] \tag{11}$$

The dimensions of the standardized data set $\boldsymbol{U}_{zs}$ are consistent with the dimensions of the original voltage data set $\boldsymbol{U}$.

2) Feature extraction based on PCA

PCA algorithm is an unsupervised dimensionality reduction algorithm based on linear transformation [29]. It uses orthogonal transformation to transform correlated variables

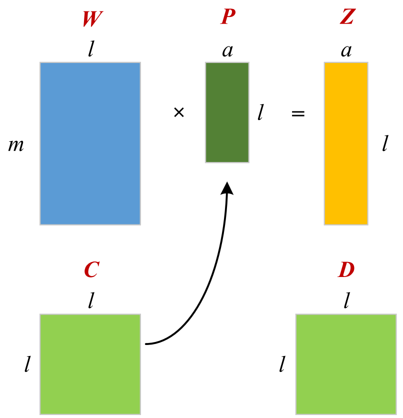

FIGURE 4. Schematic diagram of PCA.

into a group of linearly unrelated variables, so as to obtain the main content that can replace the data and achieve dimensionality reduction and feature extraction by abandoning other minor dimensions.

PCA is widely used to eliminate data redundancy and data noise. The schematic diagram of PCA is shown in Fig.4. In Fig.4, $\boldsymbol{W}$ is original data matrix of dimension $m\times l$, $\boldsymbol{C}$ is the covariance matrix of $\boldsymbol{W}$, $\boldsymbol{P}$ is the transformation matrix of dimension $l\times a$, a is the number of principal components to be retained, $\boldsymbol{Z}$ is the matrix after dimensionality reduction; $\boldsymbol{D}$ is the covariance matrix of $\boldsymbol{Z}$.

Perform PCA dimensionality reduction processing on the voltage standardized data set $\boldsymbol{U}_{zs}$, then obtain a data matrix $\boldsymbol{U}_{zs}{}'$ of dimension $N\times a$, which retains $a-$dimensional main feature, where N is the total number of measurement points.

B. UTCR RECOGNITION MODEL BASED ON PRIOR KNOWLEDGE

There are two problems to be solved in the UTCR identification: 1) which users' UTCR are error; 2) what the real UTCR of the users with the error are. **Prior knowledge 1** and **2** mentioned in Section II contain voltage correlation characteristics of users at different LVDN. Hence, in this section, **Prior knowledge 1** and **2** are combined to build the UTCR recognition model to verify the users with the UTCR error and their real UTCR. The details are shown as follows.

Step 1: Calculate the PCCVP between measurement points on the basis of matrix $\boldsymbol{U}_{zs}{}'$, and obtain the PCCVP matrix $\boldsymbol{R}$, which can be divided into four block matrices, as shown as below.

$$R = \begin{bmatrix} R_1 \ R_2 \\ R_3 \ R_4 \end{bmatrix} \tag{12}$$

Where, $\boldsymbol{R}_1$ is an square matrix with dimension $N_1\times N_1$, which represents the PCCVP between the low-voltage bus of the LVDN to be identified and the low-voltage bus of LVDN adjacent to it, N_1 represents the total number of low-voltage buses of the LVDN to be identified and the adjacent LVDN; $\boldsymbol{R}_2$ is a matrix with dimension $N_1\times N_2$, which represents the PCCVP between the users and the low-voltage buses; $\boldsymbol{R}_3$ is a matrix with dimension $N_2\times N_1$, which is the transpose of the matrix $\boldsymbol{R}_2$; $\boldsymbol{R}_4$ is an square matrix with dimension $N_2\times N_2$, which represents the PCCVP between the users contained in LVDN to be recognized and adjacent LVDN; N_2 represents the total number of users of the LVDN to be identified and the neighboring LVDN.

Step 2: The column vectors in $\boldsymbol{R}_2$, described as $\boldsymbol{R}_2(:,h)$, h =1,2…,N_2 is the PCCVP value between the user h and low-voltage buses of multi-LVDNs. For the user h, the LVDN which the low-voltage bus corresponding to the maximum value in $\boldsymbol{R}_2(:, h)$ connect to is used as its initial UTCR.

Step 3: Compare the existing UTCR stored in DCU of LVDNs with the initial UTCR obtained in step 2. For the $g-$th LVDN, $g = 1, 2, \ldots, b$, b is the number of LVDN, if the users in it with inconsistent results in the comparison, these users are treated as suspected meter and form suspected user set ξ_g. After this, we obtain a total of b suspected user sets.

The larger the voltage amplitude of the user is, the closer it is to the low-voltage bus. On this basis, a location index ζ is developed to determine the users close to distribution transformer.

Step 4: For each LVDN, perform the following steps. 4-1) Average users' voltage value during measurement period by

$$U^{u}_{\text{ave}} = (\sum_{t=1}^{T} U^{t}_{u})/T \ (13) \tag{13}$$

where, $U^{u}_{ave}$is the average voltage value of consumer $u$in the measurement period, $T$is the number of intervals in the measurement period.

4-2) Sort the users by average voltage value obtained in above from the highest to the lowest. The sorting result reflects the sorting of users by electrical distance between users and the low-voltage buses from nearest to farthest.

4-3) $\zeta_g = \lceil \tau * M_g \rceil$, τ is a threshold coefficient, $\tau \in [0,0.5]$, M_g is the number of users stored in the DCU of the g-th LVDN. The value of τ is related to the three-phase voltage unbalance and smart meter incomplete ratio in LVDN. Further, extract top ζ_g users from the sorted result in step 4-2) to form set η_g as the set of consumers near the low-voltage buses in the g-th LVDN. After this, we obtain a total of b consumer sets near the low-voltage buses.

Step 5: Let E_g=$\xi_g \cap \zeta_g$, the users in set E_g represent the users both exist in the sets ξ_g and ζ_g. Their UTCR are erroneous and are modified as the results in step 2). These users are further removed from the set ξ_g, and ξ_g is updated to ξ_{1g}, g= 1, 2, …, b.

Step 6: Divide the users in each LVDN into a set of suspected users and a set of non-suspected users. For example, the set of suspected users and the set of non-suspected users in the g-th LVDN are represented by ξ_{1g} and λ_{1g} respectively. For each user in set ξ_{1g}, extract the PCCVP value between it and non-suspected users in the LVDNs from the matrix $\boldsymbol{R}_4$. Each user has a total of b voltage correlation coefficient series. The g-th voltage correlation coefficient series of the

k-th in $\xi_{1g}$is described as $\boldsymbol{R}_{k,gg}$, as shown as follows.

$$R_{k,gg} = \{\rho_{1\ gk,1g1}, \rho_{1\ gk,1g2}, \ldots \rho_{1\ gk,1go}, \ldots, \rho_{1\ gk,1gO}\} \tag{14}$$

where, $\rho_{1gk,1go}$are the PCCVP value between the $k-$th user in ξ_{1g} and the $o-$th user in λ_{1g}, o represents the number of users in the set λ_{1g}, $g = 1,2, \ldots, b$.

Step 7: Calculate the mean value $\boldsymbol{E}_{1g,k}$ and standard deviation series $\boldsymbol{F}_{1g,k}$ of b voltage correlation coefficient series of the $k-$th user in ξ_{1g}, namely, based on $\boldsymbol{R}_{k,gg}$.

$$E_{1\ g,k} = \left\{\mu_{kg1}, \mu_{kg2}, \ldots, \mu_{kgv}, \ldots, \mu_{kgb}\right\} \tag{15}$$

$$F_{1\ g,k} = \left\{\sigma_{kg1}, \sigma_{kg2}, \ldots, \sigma_{kgv}, \ldots, \sigma_{kgb}\right\} \tag{16}$$

where, μ_{kgv} and σ_{kgv} are the mean value and standard deviation of the $v-$th voltage correlation coefficient sequence of the $k-$th user in ξ_{1g}, respectively, $v = 1, 2, \ldots, b$, $g = 1, 2, \ldots, b$.

For the $k-$th user in ξ_{1g}, if the μ_{kgv} and σ_{kgv} of the $v-$th LVDN are both greater than μ_{kgg} and σ_{kgg} of the $g-$th LVDN, its UTCR is erroneous and is corrected to connect to the $v-$th LVDN, otherwise its UTCR is subjected to results in step 2, $g = 1, 2, \ldots, b$.

V. CASE STUDY

The proposed method was modelled in MATLAB R2019a. Simulations for case study were run on 11th Gen Intel(R) Core (TM) i5-1135G7 @ 2.40GHz with 16.0 GB memory. The case study includes five parts. At first, the data used in case study are described. Then, the identification procedure is given to show how the proposed method identifies the consumer phase in detail. Further, the performance of the proposed method is evaluated. After that, the comparisons between the proposed method and other published methods are carried out. Finally, the influence of the number of principal components defined in Section III.A on the identification accuracy is investigated.

A. DATA DESCRIPTION FOR CASE STUDY

In order to verify the effectiveness of the proposed method, two LVDNs model based on real LVNDs in Guangdong are established in MATLAB to simulate the adjacent LVDN scenario. The connectivity of two adjacent LVDN on 10kV line is shown in Fig.5, and the network topology of two LVDN are shown in Fig.6 and Fig.7.

The LVDN1 has 9 low-voltage feeders and serves 170 consumers including 150 single-phase consumers and 20 three-phase consumers. The LVDN2 has 9 low-voltage feeders and serves 315 consumers including 274 single-phase consumers and 41 three-phase consumers. The smart meter in three-phase consumers can record the power consumption, voltage, current of each phase. Hence, a three-phase consumer can be treated as three single-phase consumers. In other words, there are 210 single-phase consumers in the LVDN1 and 397 single-phase consumers in the LVDN2. In two LVDNs, BLV$-$ 150×4 overhead wire is used in the feeders, BLV$-$50×2 overhead wire is used in branch lines, and BLV$-$16×2 overhead wire is used in the service drop line between feeder and household.

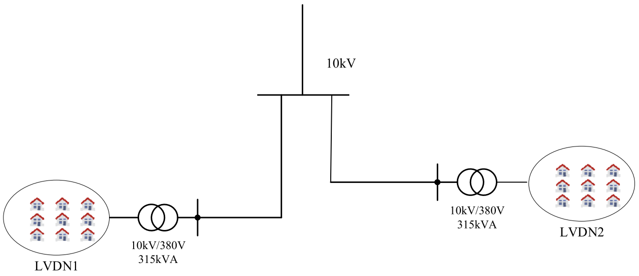

FIGURE 5. Diagram of adjacent LVDNs on 10kV line.

Based on the three-phase four-wire power flow calculation method proposed in [30], the voltage database of low-voltage buses and users of two LVDNs are obtained. Of which, load data of users in Guangdong are used in this power flow calculation.

B. IDENTIFICATION PROCEDURE

The 1-day voltage measurement data with 96 measurements of users and low-voltage buses of two LVDNs are taken from the database in this case. The user number in LVDN1 and LVDN2 starts with G and H, respectively. The UTCR of LVDN1 is set to be recognized. Assuming that there are 10 users in the adjacent LVDN2 mixed into the LVDN1's DCU file, the user names are H3, H5, H10, H12, H20, H32, H55, H56, H70, H120, respectively, to simulate the scenario with UTCR errors in LVDN. Further, set the PCA retained feature dimension $a = 30$, and the threshold parameter defined in step 4-3) of Section III.B $\tau = 0.3$.

In the simulated UTCR error scenario, treating the three-phase consumer as three single-phase consumers, there are a total of 220 single-phase meters in LVDN1, and a total of 387 single-phase meters in LVDN2. At first, construct the original voltage data matrix $\boldsymbol{U}$ according to the method described in Section III.A. $\boldsymbol{U}$ is a 613 × 96$-$dimensional matrix, in which the first six rows of elements are the low-voltage bus voltage timing data of LVDN1 and LVDN2, and the remaining elements are voltage timing data of users in two LVDNs. Then, the original voltage data matrix $\boldsymbol{U}$ was standardized and feature extracted by Z-Score normalization method and PCA dimensionality reduction method described in Section III.A, and a 613 × 30$-$dimensional data matrix $\boldsymbol{U}_{zs}{}'$ is obtained. On this basis, the PCCVP matrix $\boldsymbol{R}$ of metering points is calculated, and the preliminary UTCR of two LVDN is obtained from Step 1 and Step 2 in Section III.B.

In this initial UTCR, 210 users of LVDN1 except H3, H5, H10, H12, H20, H32, H55, H56, H70 and H120 connect to LVDN1, and 387 users of LVDN2 connect to LVDN2. The PCCVP values between the above 10 users and the 6 low-voltage buses in the two LVDNs are given in Tab.1. Where, B1$\sim$B3 are low-voltage buses of LVDN1 with phase A, B and C, respectively, B4$\sim$B6 are low-voltage buses of LVDN2

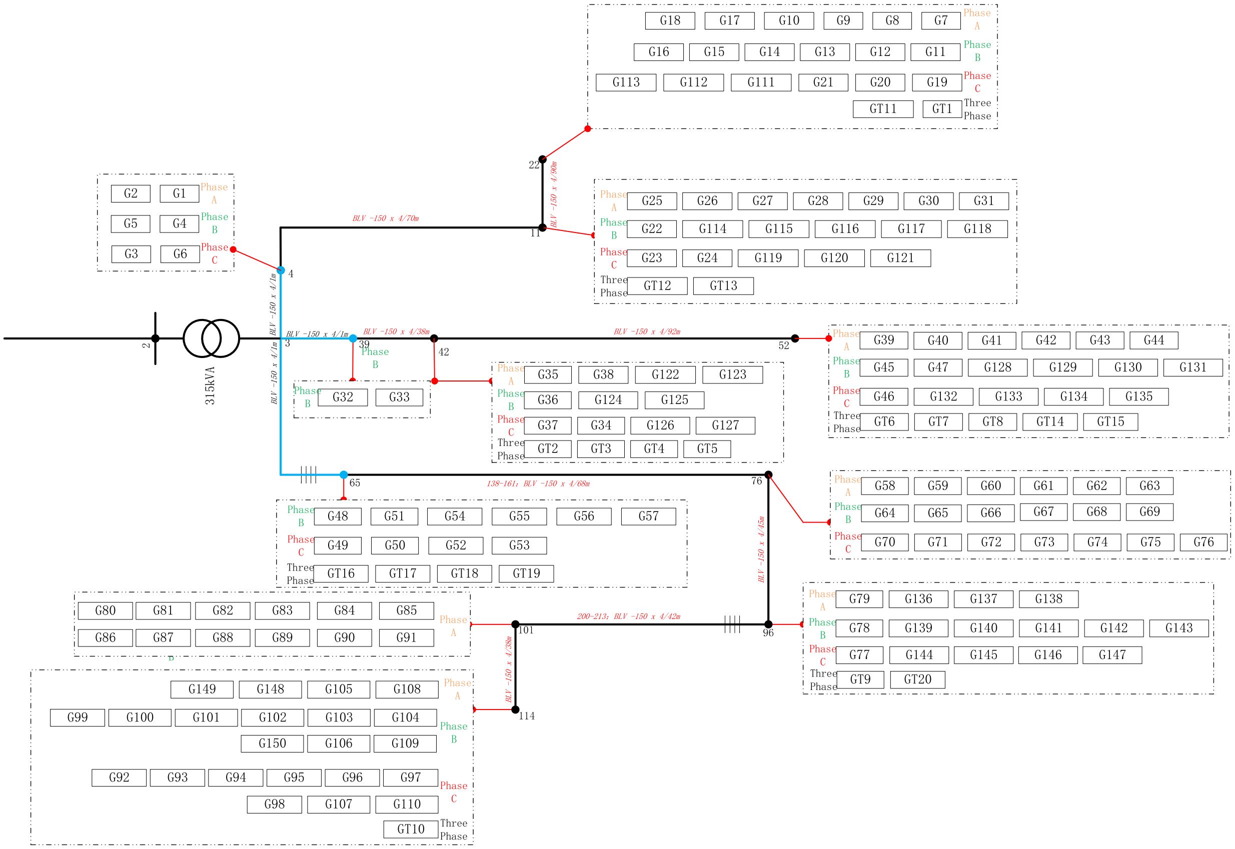
G18 G17 G10 G9 G8 G7 Phase A
G16 G15 G14 G13 G12 G11 Phase B
G113 G112 G111 G21 G20 G19 Phase C
GT11 GT1 Three Phase
22
BLV -150 x 4/90m
11
BLV -150 x 4/70m
G2 G1 Phase A
G5 G4 Phase B
G3 G6 Phase C
4
BLV -150 x 4/1m
Phase A G25 G26 G27 G28 G29 G30 G31
Phase B G22 G114 G115 G116 G117 G118
Phase C G23 G24 G119 G120 G121
Three Phase GT12 GT13
2
315kVA
BLV -150 x 4/1m
3
39
BLV -150 x 4/38m
42
BLV -150 x 4/92m
52
Phase B
Phase B G32 G33
Phase A G35 G38 G122 G123
Phase B G36 G124 G125
Phase C G37 G34 G126 G127
Three Phase GT2 GT3 GT4 GT5
Phase A G39 G40 G41 G42 G43 G44
Phase B G45 G47 G128 G129 G130 G131
Phase C G46 G132 G133 G134 G135
Three Phase GT6 GT7 GT8 GT14 GT15
65
138-161: BLV -150 x 4/68m
76
Phase B G48 G51 G54 G55 G56 G57
Phase C G49 G50 G52 G53
Three Phase GT16 GT17 GT18 GT19
Phase A G58 G59 G60 G61 G62 G63
Phase B G64 G65 G66 G67 G68 G69
Phase C G70 G71 G72 G73 G74 G75 G76
BLV -150 x 4/46m
G80 G81 G82 G83 G84 G85 Phase A
G86 G87 G88 G89 G90 G91
101
200-213: BLV -150 x 4/42m
96
Phase A G79 G136 G137 G138
Phase B G78 G139 G140 G141 G142 G143
Phase C G77 G144 G145 G146 G147
Three Phase GT9 GT20
BLV -150 x 4/38m
114
G149 G148 G105 G108 Phase A
G99 G100 G101 G102 G103 G104 Phase B
G150 G106 G109
G92 G93 G94 G95 G96 G97 Phase C
G98 G107 G110
GT10 Three Phase

FIGURE 6. Diagram of LVDN1 network topology.

TABLE 1. PCCVP value between 10 users and 6 low-voltage buses.

Users	Low-voltage buses					
	B1	B2	B3	B4	B5	B6
H3	0.770	0.772	0.770	0.782	0.716	0.727
H5	0.744	0.744	0.744	0.696	0.768	0.764
H10	0.918	0.906	0.875	0.948	0.884	0.835
H12	0.925	0.914	0.887	0.955	0.894	0.849
H20	0.587	0.611	0.628	0.537	0.612	0.656
H32	0.576	0.572	0.588	0.546	-0.607	-0.610
H55	0.295	0.287	0.243	0.343	0.246	0.193
H56	0.319	0.312	0.267	0.368	0.270	0.219
H70	0.880	0.871	0.840	0.910	0.847	0.803
H120	0.889	0.880	0.847	0.919	0.855	0.810

with phase A, B and C, respectively. And the value marked in red is the maximum CCVP between user and low-voltage buses.

It can be seen from Tab.1 that the low-voltage buses with the largest PCCVP value of user H3, H5, H10, H12, H20, H32, H55, H56, H70, H120 all belong to LVDN2. However, the ID information of these 10 users is in LVDN1. In other words, for these 10 users, the existing UTCR stored in DCU of LVDNs and the initial UTCR obtained by Step 2 in Section III.B are inconsistent, so these 10 users are included in the suspected user set ξ_1. Further, perform Step 4 in Section III.B, two consumer sets near the low-voltage buses are obtained, as shown in Tab.2.

It can be seen from Tab.2 that the above 10 suspected users are not in consumer sets near the low-voltage buses. According to Step 5 in Section III.B, the updated suspected user set ξ_{11} is still equal to the set of suspected users set ξ_1. Then, perform Step 6 and Step 7 in Section III.B for these 10 suspected users and the mean value $\boldsymbol{E}_{1g}$ and standard deviation series $\boldsymbol{F}_{1g}$ are obtained, as shown in Tab.3.

It can be seen from Tab.3 that the mean and standard deviation of PCCVP values between the 10 suspected user and non-suspected users in the LVDN2 are higher than those in LVND1. Therefore, these 10 suspected users are confirmed as users with wrong UTCR, and their real UTCR is connected to LVDN2. The recognition result is consistent with the real situation, and the recognition accuracy is 100%, which fully verifies the effectiveness and accuracy of the proposed method.

C. PERFORMANCE EVALUATION OF THE PROPOSED METHOD

In this section, the performance of the proposed method under the conditions of different UTCR error rate, data measurement error rate, three-phase imbalance level and data length

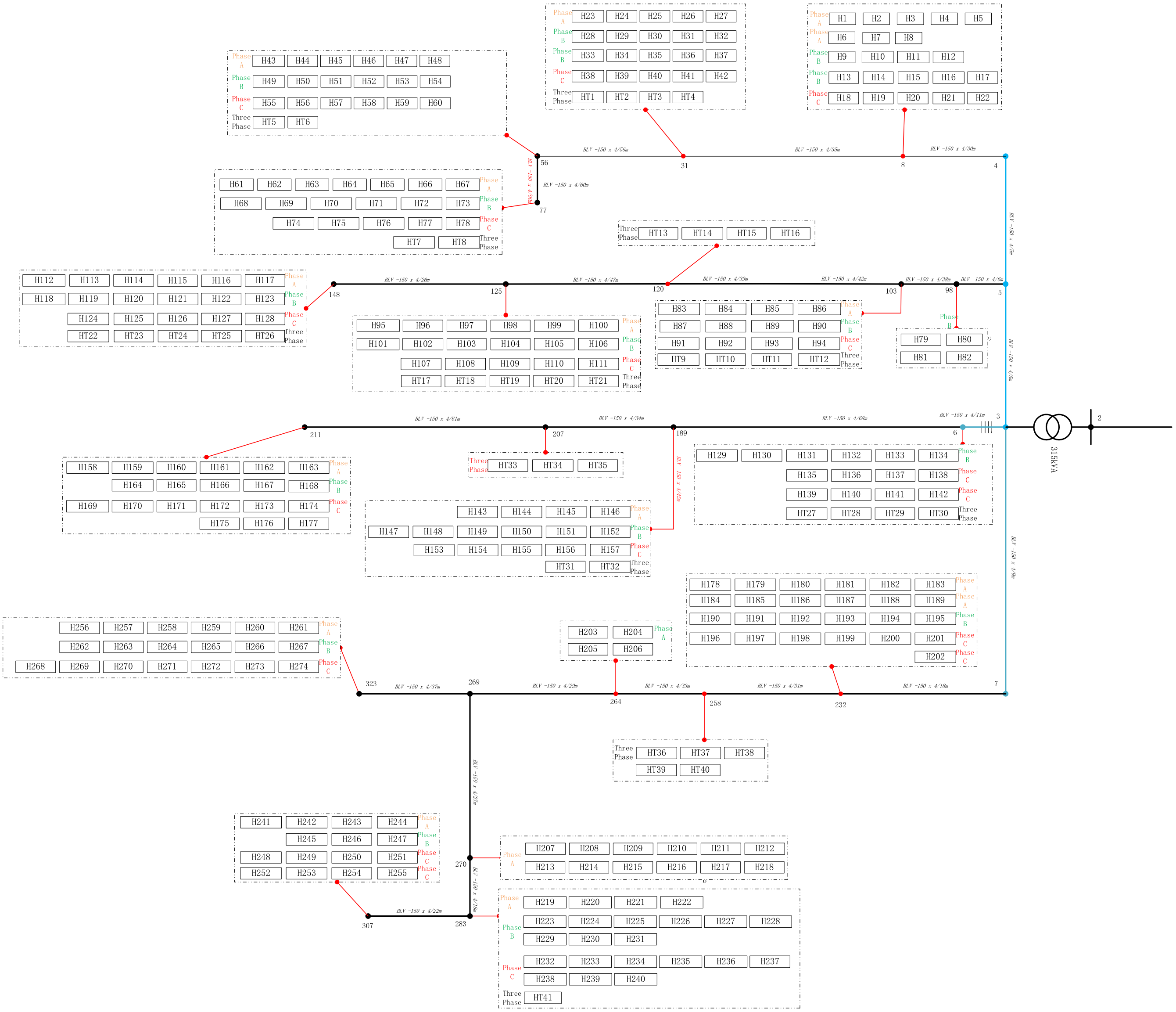

FIGURE 7. Diagram of LVDN2 network topology.

TABLE 2. User sets of two lvdns near the low-voltage buses.

LVND	User sets
LVDN1	G1,G2,G199,G205,G202,G196,G154,G16,G160,G157,G163,G17,G46,G45,G52,G61,G53,G3,G62,G9,G67,G68,G66,G4,G184,G5,G203,G69,G70,G187,G6,G197,G200,G206,G71,G8,G7,G105,G104,G114,G115,G116,G117,G198
LVDN2	H346,H349,H343,H352,H355,H358,H39,H38,H40,H37,H344,H350,H353,H347,H138,H136,H51,H141,H139,H52,H49,H53,H137,H48,H55,H50,H54,H47,H56,H119,H1,H2,H116,H118,H117,H367,H361,H364,H5,H3,H4,H6,H289,H298,H292,H295,H22,H24,H23,H25,H44,H43,H42,H153,H41,H46,H45,H154,H158,H155,H156,H157,H345,H212,H213,H351,H348,H354,H217,H214,H216,H218,H215,H219,H140,H265,H271

are investigated. In detail, by increasing the number of users in LVDN2 into the DCU reading file of LVDN1, the data scenario with increasing UTCR error rate is constructed. UTCR error rate ε is defined as the ratio of the number of users not belonging to LVDN1 to the total number of LVDN1 users, as below.

$$\varepsilon = \frac{N_{\text{false}}}{N_{\text{LVDN1}}} \tag{17}$$

where, N_{false} is the number of users not belonging to LVDN1, N_{LVDN1} is the total number of LVDN1 users.

To construct the data scenario with an increasing data measurement error rate η, every user's measurement has been added noise by introducing a Gaussian error whose mean value is 0 and standard deviation is one third of the measurement error rate η.

Λ is set as the average value of three-phase voltage unbalance in the measurement period to reflect the three-phase

TABLE 3. The $E_{1g}$and $F_{1g}$of PCCVP values between the suspected user and non-suspected users in the two LVDN.

User	E_{1g}			F_{1g}		
	LVDN 1	LVDN 2	difference	LVDN 1	LVDN 2	difference
H3	0.067	0.224	-0.156	0.071	0.245	-0.174
H5	0.091	0.299	-0.207	0.071	0.264	-0.192
H10	0.113	0.328	-0.215	0.069	0.216	-0.148
H12	0.103	0.334	-0.231	0.056	0.217	-0.161
H20	0.133	0.258	-0.125	0.073	0.245	-0.172
H32	0.092	0.202	-0.110	0.067	0.223	-0.156
H55	0.094	0.236	-0.142	0.061	0.217	-0.156
H56	0.098	0.238	-0.141	0.064	0.216	-0.152
H70	0.084	0.268	-0.184	0.049	0.188	-0.139
H120	0.087	0.280	-0.193	0.052	0.184	-0.131

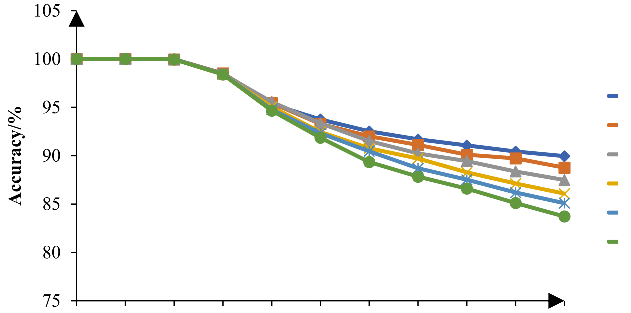

FIGURE 8. UTCR identification accuracy under different ε and η.

unbalance level of LVDN, as described below.

$$\Lambda = [\sum_{t=1}^{T} \frac{U_D^{\max}(t) - U_D^{\min}(t)}{U_D^{\max}(t)} \times 100\%]/T \tag{18}$$

where, $U_D^{max}(t)$ is the maximum voltage in low-voltage buses at time t, $U_D^{min}(t)$ is the minimum voltage in low-voltage buses at time t, T is the number of intervals in a measurement period.

Firstly, a comprehensive calculation is executed by gradually increasing the value of ε and η with fixed data length (15 days with 1440 measurements). Under each data scenario, UTCR identification is executed multiple times to obtain average accuracy. The results are shown as below.

As shown in Fig.8, with the fixed ε value, as the measurement error rate η increases, the recognition accuracy rate decreases. When η is less than 0.4%, the recognition accuracy of the proposed method drops slightly, which is close to 100%. When $\eta > 0.4\%$, the recognition accuracy rate is greatly affected by the measurement error. When η is in the interval of [0.4%, 1%], the downward slope is large. In addition, the increase in η will magnify the impact of UTCR error rate ε on the recognition accuracy. For example, when η is less than 0.4%, the difference in the recognition accuracy of the six scenarios with different ε value is very small, and the recognition accuracy are all close to 100%. When η exceeds 0.4%, the recognition accuracy difference of the six scenarios with different ε value becomes larger as η increases. And the higher ε is, the lower the recognition accuracy rate.

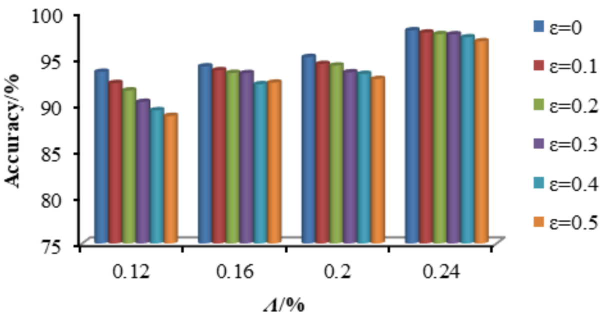

FIGURE 9. UTCR identification accuracy under different ε and Λ.

This is because the core of the proposed method is to compare the PCCVP values between measurement points. The superposition of measurement errors changes the PCCVP value between different voltage curves. Specifically, the similarity of voltage curves between users and the connected low-voltage buses, and that between users located in the same LVDN is reduced. At this time, it's uncertain which low-voltage bus has the largest CCVP value with them. In other words, the LVDN where the low-voltage bus having the largest CCVP value to them is located may be same or different from the LVDN them are connected to, on a case-by-case basis.

Then, a comprehensive calculation is executed by gradually increasing the value of ε and Λ with fixed data length (15 days with 1440 measurements) and fixed measurement error rate of 0.4%. Under each data scenario, UTCR identification is executed multiple times to obtain average accuracy. The results are shown as below.

As shown in Fig.9, with fixed Λ value, the identification accuracy increases gradually as Λ increases. The reason is that the proposed method depends on the PCCVP value among users and that between consumers and low-voltage buses of LVDN. As three-phase imbalance level (Λ) increases, the voltage discrimination of users connected to different phases increases so that the identification accuracy of the proposed method is gradually improved. In particular, in the scenario where the ε is 0.5, the recognition accuracy rate is increased by 8% when the Λ is 0.24% compared with when the Λ is 0.12%. Therefore, in order to alleviate the influence of measurement error, the data in the period with large three-phase imbalance level can be selected to carry out UTCR identification.

Further, the influence of data length is discussed. A comprehensive calculation is executed by gradually increasing the value of η and length of data with fixed UTCR error rate of 0.3. Under each data scenario, UTCR is executed multiple

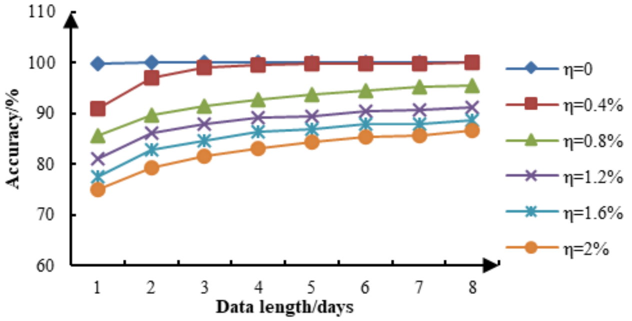

FIGURE 10. UTCR identification accuracy under different data length and η.

times to obtain average accuracy. The results are shown in Fig.10.

It can be seen from Fig.10 that when there is no data measurement error ($\eta = 0$), the recognition accuracy rate for each data length is 100%. When there is a data measurement error ($\eta = 0.4\% \sim 2\%$), the recognition accuracy rate increases as the data length increases, and the growth rate gradually slows down. This is because the difference in the PCCVP value between users increases with the increase of the data length, thereby improving the recognition accuracy. In particular, when $\eta = 0.4\%$, the recognition accuracy in the data scenario of 6-8 days can be increased to 100%. Therefore, in order to alleviate the influence of the measurement error, the data with a longer time length can be selected for UTCR recognition.

D. COMPARISON ANALYSIS WITH OTHER PUBLISHED METHODS

In this section, multiple data scenarios are constructed by gradually increasing the value of ε and η with fixed data length of one day to compare the performance of different methods. At present, there are two methods to identify UTCR based on AMI measurement data. One is to compare voltage curve correlation between users [22], and the other is to compare voltage curve correlation between users and low-voltage buses [23]. The comparative analysis of the following four identification methods is executed.

Method 1: comparing voltage curve correlation between users [22];

Method 2: comparing voltage curve correlation between users and low-voltage buses [23];

Method 3: removing Z-score standardization processing and PCA feature extraction from the proposed method;

Method 4: the proposed method.

The UTCR recognition accuracy rates of the four methods under different ε and η are shown in below.

As illustrated in Fig.11, several findings are:

1) Comparing Method 1 and Method 4, when the data measurement error $\eta = 0$, the recognition accuracy of the two methods is both 100%. But when there is a measurement error i.e., $\eta = 0.8\%$, $\eta = 1.6\%$, the recognition accuracy of Method 4 is significantly higher than that of Method 1 in every scenario. This indicates that it is not enough to accurately identify UTCR by comparing the voltage curve correlation alone when there is measurement error in data. On the basis of Method1, Method 4 taking the correlation between users as supplementary verification has better performance.

2) Comparing Method 2 and Method 4, when the data measurement error $\eta = 0$ and ε is less than 0.2, the recognition accuracy of the two methods is both 100%. However, when ε is greater than 0.2, the recognition accuracy of Method 2 decreased obviously with the increase of η, while that of Method 4 remained at 100%. The reason is that Method 2 identify UTCR by comparing the voltage curve correlation between users. When there are many users in LVDN

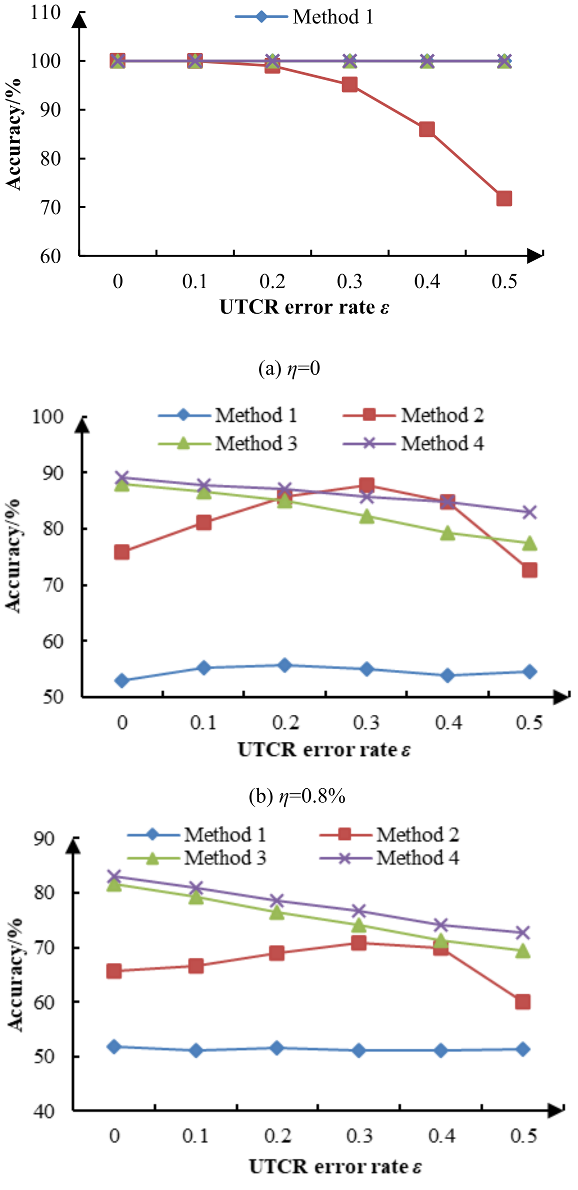

(a) η=0

(b) η=0.8%

(c) η=1.6%

FIGURE 11. Recognition performance of 4 methods in different scenarios.

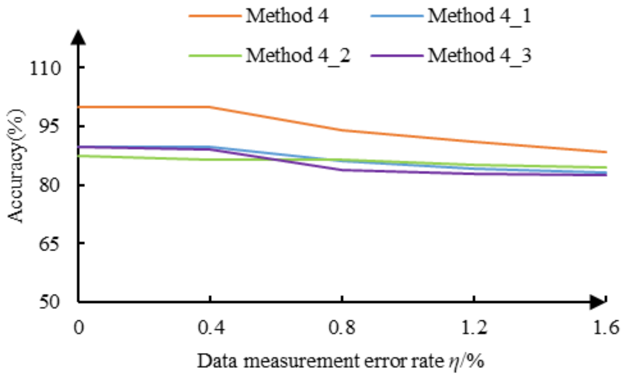

FIGURE 12. Recognition accuracy of 4 methods with different data processing link under different η.

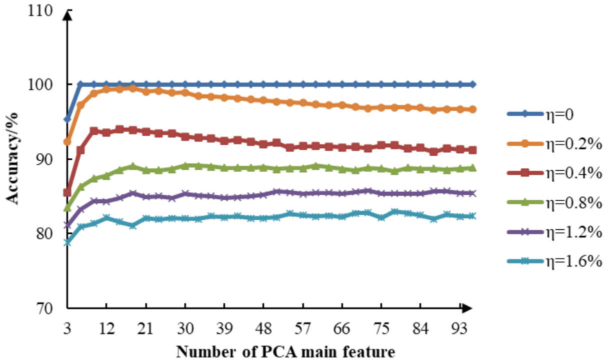

FIGURE 13. Recognition accuracy under different η and PCA main feature values.

that do not belong to it, it is easy for Method 2 to identify these users wrongly. The more users who do not belong to LVDN in the initial meter reading file of LVDN, the higher the error recognition rate of Method 2. When there is data measurement error in LVDN, there is no linear relationship between recognition accuracy and UTCR error rate in Method 2. This is because the superposition of measurement errors changes the PCCVP value between different voltage curves. Specifically, the similarity of voltage curves between users located in the same LVDN is reduced. In this case, the results of Method 2 are stochastic. Except for the scenario where $\eta = 0.8\%$ and $\varepsilon = 0.3$, the accuracy of Method 4 is higher than that of Method 2 in every scenario. This demonstrates that the recognition accuracy of Method 4 is more stable and superior.

3) Comparing Method 3 and Method 4, when the data measurement error $\eta = 0$, the recognition accuracy of the two methods is both 100%. But when there are measurement errors i.e., $\eta = 0.8\%$, $\eta = 1.6\%$, the recognition accuracy of Method 4 is higher than that of Method 3 in all scenarios. This fully illustrate that the Z-score and PCA dimensionality reduction links enhance the robustness of the recognition method against data measurement errors.

Further, to show the role of data processing in the proposed method clearly, the comparation analysis about the identification results with and without data standardization and with different dimensionality reduction techniques are carried out. Define the proposed method without data standardization as Method 4_1, the proposed method with T-SNE dimensionality reduction as Method 4_2, the proposed method without PCA dimensionality reduction as Method 4_3. Multiple data scenarios are constructed by gradually increasing the value of data measurement error rate η with UTCR error rate of 0.3 to compare the identification results, as shown in Fig.12.

As shown in Fig.12, the recognition accuracy of Method 4 with Z-score standardization and PCA dimensionality reduction is higher than that of other 3 Methods in all scenarios. Comparing Method 4_1 and Method 4_3 with Method 4, it is clearly that Z-score standardization and PCA dimensionality reduction are beneficial to improve the robustness of the recognition method against data measurement errors, respectively. And PCA dimensionality reduction perform better than T-SNE dimensionality reduction method comparing Method 4_2 and Method 4.

E. SENSITIVITY ANALYSIS FOR THE THRESHOLD COEFFICIENT

In this section, a comprehensive calculation is executed by gradually increasing the value of η and PCA main feature numbers a with fixed UTCR error rate of 0.3 and data length of one day. The results are shown as below.

It can be seen from Fig.13 that the number of PCA main features have different effects on the recognition accuracy with different η. When η=0, the increase in the number of PCA main features can increase the recognition accuracy to 100%. When $0 < \eta \leq 0.4\%$, the recognition accuracy first increases and then decreases with the increase of the number of PCA main features. When $\eta \geq 0.8\%$, the recognition accuracy first increases with the increase of the number of PCA main features and then tended to be flat. This demonstrates that the number of PCA main features for optimal recognition accuracy is affected by the measurement error rate, and the higher the measurement error rate, the greater the number of PCA main features is needed. The above results verify the effectiveness of the PCA dimensionality reduction method on retaining a few main features to replace high-dimensional data.

VI. CONCLUSION

To identify UTCR intelligently and strengthen the algorithm's robustness to data discrimination and noise, in this paper, statistical data processing methods and the prior knowledge of voltage correlation characteristics in LVDN are combined to develop a knowledge-driven UTCR identification method. The performance of the proposed method is evaluated under various conditions and compared with other published methods. Further, the influence of PCA main feature numbers is investigated. From the study, the conclusions are elaborated as follows.

1) The proposed method can effectively distinguish the users with wrong UTCR and identify their correct UTCR. The data processing process with Z-score and PCA feature extraction can enhance the robustness of the proposed method to the data measurement error.
2) The recognition accuracy of the proposed method decreases as UTCR error rate and measurement error rate increase. However, it can be improved by selecting data with high three-phase voltage imbalance level or long length.
3) In the scenario where there is measurement error in data, the proposed method outperforms the method in reference [23] that only compares the voltage curve correlation between users and low-voltage buses and the method in reference [22] that only compares the voltage curve correlation between users.
4) The number of PCA main features to achieve the best recognition accuracy is affected by the measurement error rate, and the higher the measurement error rate, the greater the number of PCA main features is needed.

The probability to reverse power flow on LVDN will be increased as the penetration of renewable micro-generation such as photovoltaic increases. Thus, how to recognize UTCR with the reverse power flow will be investigated in the future.

REFERENCES

[1] X. Chen and B. Lin, "Towards carbon neutrality by implementing carbon emissions trading scheme: Policy evaluation in China," *Energy Policy*, vol. 157, Oct. 2021, Art. no. 112510.

[2] X. Wu, Z. Tian, and J. Guo, "A review of the theoretical research and practical progress of carbon neutrality," *Sustain. Oper. Comput.*, vol. 3, pp. 54–66, Jan. 2022.

[3] L. Zhou, Y. Zhang, X. Lin, C. Li, Z. Cai, and P. Yang, "Optimal sizing of PV and BESS for a smart household considering different price mechanisms," *IEEE Access*, vol. 6, pp. 41050–41059, 2018.

[4] L. Dong, C. Wang, M. Li, K. Sun, T. Chen, and Y. Sun, "User decision-based analysis of urban electric vehicle loads," *CSEE J. Power Energy Syst.*, vol. 7, no. 1, pp. 190–200, Jan. 2021.

[5] C. Byers and A. Botterud, "Additional capacity value from synergy of variable renewable energy and energy storage," *IEEE Trans. Sustain. Energy*, vol. 11, no. 2, pp. 1106–1109, Apr. 2020.

[6] F. M. Camilo, R. Castro, M. E. Almeida, and V. F. Pires, "Probabilistic load elasticity analysis in low voltage distribution networks with high penetration of photovoltaic micro generation," *Int. J. Electr. Power Energy Syst.*, vol. 113, pp. 782–791, Dec. 2019.

[7] Y. He, M. Wang, Y. Jia, J. Zhao, and Z. Xu, "Low-voltage ride-through control for photovoltaic generation in the low-voltage distribution network," *IET Renew. Power Gener.*, vol. 14, no. 14, pp. 2727–2737, Oct. 2020.

[8] B. Liu, K. Meng, Z. Y. Dong, P. K. C. Wong, and T. Ting, "Unbalance mitigation via phase-switching device and static var compensator in low-voltage distribution network," *IEEE Trans. Power Syst.*, vol. 35, no. 6, pp. 4856–4869, Nov. 2020.

[9] S. J. Pappu, N. Bhatt, R. Pasumarthy, and A. Rajeswaran, "Identifying topology of low voltage distribution networks based on smart meter data," *IEEE Trans. Smart Grid*, vol. 9, no. 5, pp. 5113–5122, Sep. 2018.

[10] M. Lave, M. J. Reno, and J. Peppanen, "Distribution system parameter and topology estimation applied to resolve low-voltage circuits on three real distribution feeders," *IEEE Trans. Sustain. Energy*, vol. 10, no. 3, pp. 1585–1592, Jul. 2019.

[11] L. Ping, Y. Yonghui, X. Mingzhu, L. Fei, W. Jinran, L. Xinran, L. Ling, and S. Guoqiang, "The reaserch of users-transformer relationship verification method based on data-driven," in *Proc. IEEE Innov. Smart Grid Technol.-Asia (ISGT Asia)*, May 2019, pp. 2550–2554.

[12] M. Lisowski, R. Masnicki, and J. Mindykowski, "PLC-enabled low voltage distribution network topology monitoring," *IEEE Trans. Smart Grid*, vol. 10, no. 6, pp. 6436–6448, Nov. 2019.

[13] P. Van Aubel and E. Poll, "Smart metering in The Netherlands: What, how, and why," *Int. J. Electr. Power Energy Syst.*, vol. 109, pp. 719–725, Jul. 2019.

[14] J. B. Leite and J. R. S. Mantovani, "Detecting and locating non-technical losses in modern distribution networks," *IEEE Trans. Smart Grid*, vol. 9, no. 2, pp. 1023–1032, Mar. 2018.

[15] Y. Wang, Q. Chen, T. Hong, and C. Kang, "Review of smart meter data analytics: Applications, methodologies, and challenges," *IEEE Trans. Smart Grid*, vol. 10, no. 3, pp. 3125–3148, May 2019.

[16] K. Soumalas, G. Messinis, and N. Hatziargyriou, "A data driven approach to distribution network topology identification," in *Proc. IEEE Manchester PowerTech*, Jun. 2017, pp. 1–6.

[17] L. Zhou, Y. Zhang, S. Liu, K. Li, C. Li, Y. Yi, and J. Tang, "Consumer phase identification in low-voltage distribution network considering vacant users," *Int. J. Electr. Power Energy Syst.*, vol. 121, Oct. 2020, Art. no. 106079.

[18] L. Zhou, Q. Li, Y. Zhang, J. Chen, Y. Yi, and S. Liu, "Consumer phase identification under incomplete data condition with dimensional calibration," *Int. J. Electr. Power Energy Syst.*, vol. 129, Jul. 2021, Art. no. 106851.

[19] Y. Hu, Q. Cao, L. Wang, T. Huang, Z. Hu, and Z. Fan, "Low voltage transformer topology identification method based on de-noised differential evolution," in *Proc. 10th Int. Conf. Power Energy Syst. (ICPES)*, Dec. 2020, pp. 356–360.

[20] W. Hu, Y. Liu, Q. Guo, W. Wang, S. Song, and Y. Liu, "A data-driven method of users-transformer relationship identification in the secondary power distribution system," in *Proc. IEEE 4th Conf. Energy Internet Energy Syst. Integr. (EI)*, Oct. 2020, pp. 585–590.

[21] J. D. Watson, J. Welch, and N. R. Watson, "Use of smart-meter data to determine distribution system topology," *J. Eng.*, vol. 2016, no. 5, pp. 94–101, May 2016.

[22] W. Luan, J. Peng, M. Maras, J. Lo, and B. Harapnuk, "Smart meter data analytics for distribution network connectivity verification," *IEEE Trans. Smart Grid*, vol. 6, no. 4, pp. 1964–1971, Jul. 2015.

[23] Y. Xiao, Y. Zhao, and Z. Tu, "Topology checking method for low voltage distribution network based on improved Pearson correlation coefficient," *Power Syst. Protection Control*, vol. 47, no. 11, pp. 37–43, 2019.

[24] A. Guzman, A. Arguello, J. Quiros-Tortos, and G. Valverde, "Processing and correction of secondary system models in geographic information systems," *IEEE Trans. Ind. Informat.*, vol. 15, no. 6, pp. 3482–3491, Jun. 2019.

[25] T. A. Short, "Advanced metering for phase identification, transformer identification, and secondary modeling," *IEEE Trans. Smart Grid*, vol. 4, no. 2, pp. 651–658, Jun. 2013.

[26] W. Hu, Y. Liu, Q. Guo, J. Wang, Y. Wang, and Z. Zhao, "Detection of users-transformer relationship in the secondary power distribution system with smart meter data," in *Proc. 15th IEEE Conf. Ind. Electron. Appl. (ICIEA)*, Nov. 2020, pp. 449–454.

[27] L. Blakely and M. J. Reno, "Identification and correction of errors in pairing AMI meters and transformers," in *Proc. IEEE Power Energy Conf. Illinois (PECI)*, Apr. 2021, pp. 1–8.

[28] V. C. Cunha, W. Freitas, F. C. L. Trindade, and S. Santoso, "Automated determination of topology and line parameters in low voltage systems using smart meters measurements," *IEEE Trans. Smart Grid*, vol. 11, no. 6, pp. 5028–5038, Nov. 2020.

[29] A. Rehman, A. Khan, M. A. Ali, M. U. Khan, S. U. Khan, and L. Ali, "Performance analysis of PCA, sparse PCA, kernel PCA and incremental PCA algorithms for heart failure prediction," in *Proc. Int. Conf. Electr., Commun., Comput. Eng. (ICECCE)*, Jun. 2020, pp. 1–5.

[30] D. R. R. Penido, L. R. D. Araujo, S. Carneiro, J. L. R. Pereira, and P. A. N. Garcia, "Three-phase power flow based on four-conductor current injection method for unbalanced distribution networks," *IEEE Trans. Power Syst.*, vol. 23, no. 2, pp. 494–503, May 2008.